

<https://doi.org/10.1038/s40494-025-01627-9>

Evaluation of ecosystem carrying capacity and diagnosis of obstacle factors in the World Heritage Karst sites

**Meirong Xu, Kangning Xiong✉, Yue Chen & Mingjun Feng**

The ecosystem carrying capacity (ECC) of the karst world heritage site (KWHS) is a critical factor influencing regional development and Environmental Protection of Heritage Site (HS). However, studies on the ECC of KWHS are limited. This paper examines the Shibing and Libo-Huanjiang KWHS, utilizing 16 evaluation indices covering natural environment and socio-economic aspects. We apply subjective and objective weighting methods, cold and hot spot analysis, and the geographical detector to analyze the spatial and temporal differentiation characteristics of the ECC of KWHS from 2010 to 2020 and identify its obstructive factors. The results indicate: (1) The ECC of the KWHS core zone is significantly greater than that of the buffer zone, and the ECC of the buffer zone with no human disturbance is greater than that of the buffer zone with strong human activity from 2010 to 2020. By 2020, the Shibing HS is dominated by the Stronger ECC zone, while Libo-Huanjiang HS is dominated by the Strongest and Stronger ECC zones. (2) From 2010 to 2020, the ECC of KWHS exhibited a general downward trend, with ecological environment degradation being more pronounced in Shibing HS than in Libo-Huanjiang HS. (3) The spatial pattern of ECC in the KWHS showed strong spatial agglomeration over time, with noticeable spatial differentiation. Hot spot areas were primarily within core zone, while cold spot areas were mainly in the buffer zone. (4) Land use intensity, development disturbance index, and economic development index were the main driving factors of ECC in Shibing HS. In Libo-Huanjiang HS, ECC spatial differentiation was more influenced by ecological sensitivity and habitat quality index, with some factor interactions having a greater impact than single factors.

The accumulation of global ecological risks, the abnormal intensification of climate change, and resource shortages have led to the weakening of the ecosystem's self-regulation function, seriously threatening the sustainable development of the natural-social-economic composite ecosystem^{1,2}. Since the United Nations proposed the 2030 Sustainable Development Goals in 2015, evaluating ecosystem carrying capacity (ECC) has become a key topic in global environmental change research³. Initially, carrying capacity was applied to engineering geology⁴. With the acceleration of industrialization and urbanization, issues such as land loss and environmental pollution have continuously emerged. Consequently, the term carrying capacity has been used to describe the maximum capacity of ecosystems to withstand environmental changes^{5,6}. The concept of carrying capacity was first introduced in 1921^{7,8} and formally incorporated into ecology in 1922. With the ongoing development of the social economy, carrying capacity has become closely

linked to environmental pollution, urban congestion, population density, and ecological deterioration. The concept of carrying capacity has evolved to accommodate different research directions^{9–11}. In China, around the 1990s, scholars provided various interpretations of ECC, emphasizing the interactive system between humans and nature, the self-sustaining and self-regulating nature of ecosystems, the symbiosis and compatibility of resources and the environment, and the support for social and economic development^{12,13}. Currently, the development of carrying capacity research is in a rapid growth stage, focusing primarily on the ECC of tourism, agriculture, forestry, fisheries, and river basins^{14–17}. Numerous studies have examined ECC in karst areas; however, these studies are relatively simple, concentrating mainly on the ECC of water resources, mountain cities, and world natural heritage sites (HS) in karst mountainous regions, with less emphasis on composite ECC studies^{18,19}. With ongoing improvements in

School of Karst Science, Guizhou Normal University/State Engineering Technology Institute for Karst Desertification Control, Guiyang, Guizhou, China.

✉ e-mail: xiongkn@163.com

population quality and economic development, ECC evaluations have expanded beyond single factors and current conditions to focus on multi-factor comprehensive influences and long-term scales²⁰. Common research methods include the ecological footprint model²¹, comprehensive index method²², fuzzy comprehensive evaluation method, and technique for order preference by similarity to an ideal solution method^{23,24}. These methods are mature, practical, and produce credible results. However, practical research has revealed significant discrepancies between research results and reality due to differences in research scale and the difficulty of obtaining crucial research parameters, leading to less accurate results^{25,26}. Currently, ECC research is primarily conducted on a large scale, encompassing global countries, watersheds, urban agglomerations, and counties. Research on the ecological environment of key areas is relatively shallow, resulting in a superficial analysis of the research objects and an incomplete explanation of their ecological environment characteristics.

World heritage (WH) represents the pinnacle of human ingenuity and natural evolution²⁷. It is an irreplaceable and valuable resource with outstanding universal value^{28,29}. WH serves as an important testament to social development, geological evolution, and scientific progress, while also enhancing national pride. As of 2022, there are 167 WH contracting states, 1154 world HS, and 30 karst world heritage sites (KWHs) globally. In the South China KWHs, the core area is the KWHs and the buffer zone is its peripheral protection area^{30,31}, which can protect the integrity and sustainability of the site from threats³². According to the WH Center in 2021, 30% of the world's natural HS face threats from natural factors such as extreme weather, wildfires, and climate change, significantly impacting these sites. Human activities also pose substantial threats to WH³³. Specifically, the tourism-driven economic development spurred by the WH brand effect^{34,35} and environmental pollution have severely threatened the aesthetic value, integrity, and biodiversity protection of these sites.

China's 12 world natural HS have become major attractions for both domestic and international tourists due to their outstanding universal value^{36,37}. In terms of development conditions, degree of development, and landscape aesthetics, the karst regions in southern China are exemplary. These regions belong to the tropical-subtropical monsoon type and are listed on the WH List under criteria (vii) and (viii)^{38,39}. The unique geological formations, evolutionary processes, ecosystems, and biodiversity of the southern Chinese karst regions contribute significantly to their global value and importance^{40,41}.

The fact that KWHs are nurtured in the ecologically fragile karst region and are threatened by the threats caused by the continuous development of heritage tourism has aroused scholars' attention to the ecological conservation of KWHs. Fang et al.⁴² found that awareness of heritage values and positive tourism impacts are important for the formation of the concept of conservation responsibility among residents in the buffer zone of HS, and Zhang et al.⁴³ revealed that the habitat quality of KWHs generally maintained a better level from 2000 to 2020, and that there was a positive correlation between the habitat quality and the altitude. Zhang et al.⁴⁴ found that relatively stable land use types promoted ecosystem stability in KWHs. These studies provide relevant information about the ecosystem of the KWHs, but most of them are limited to the buffer zone only, and there are few studies on the evaluation of the ecological environment status that spatially integrates the natural, socio-economic, and tourism landscape elements.

In summary, this paper evaluates the spatial and temporal evolution trend of ECC using the comprehensive evaluation method, assesses the spatial aggregation characteristics of ECC using cold hotspot analysis, and finally explores the driving factors of ECC based on geo-detectors. The objectives of this study are to (1) assess the spatial and temporal evolution characteristics of the ECC of the KWHs from 2010 to 2020 (2) reveal the spatial agglomeration of the ECC of the KWHs (3) explore the key driving factors affecting the ECC. Investigating the ecological environment of KWHs and conducting large-scale, high-precision assessments of ECC impact factors will enhance our understanding of

the current environmental status and challenges faced by these HS. This understanding is crucial for the rational use of heritage resources, promoting the harmonious development of heritage protection and economic growth, and providing valuable insights for ecological conservation in other regions.

Materials and methods

Research area

Shi Bing KWHs. Shiping KWHs is located in the central and eastern part of Guizhou Province and the northern part of Shiping County, Qiannan Prefecture. The total area is 282.98 km², with the HS covering 102.80 km² and the buffer zone spanning 180.5 km². It is situated at coordinates 27°10'16"N, 108°05'40"E, with an average annual precipitation of 1220 mm and an average annual temperature of 16 °C. The elevation ranges from 600 to 1250 m, with an average altitude of 912 m (Fig. 1). Shiping Karst was successfully designated as a World HS in 2014. It is an exemplary representative of the world's tropical and subtropical dolomite karst, characterized by its unique geomorphological features, long evolutionary history, and diverse landforms, which significantly contribute to the integrity of the South China Karst series.

Libo - Huanjiang KWHs. The Libo-Huanjiang KWHs is situated at the junction of Libo County, Guizhou Province, and Maonan Autonomous County, Guangxi. The central coordinates are 25°12'08"N, 107°58'40"E. The HS receives an average annual precipitation of 1752 mm, with an average annual temperature of 15 °C and an average altitude of 758 m. The total area of the HS is 730.16 km², with the core area encompassing 295.18 km² (Fig. 1). Libo-Huanjiang Karst was successfully designated as a HS in 2007. It showcases the complex geological background necessary for the development of conical karst, including lithology and structure, explains the intricate history of climate evolution in this region, and preserves a variety of surface and subterranean landscapes along with unique primitive forest ecosystems. It is a quintessential representative of conical karst.

Data sources

Based on Landsat 5 TM and Landsat 8 OLI remote sensing satellite images with a band resolution of 30 m, Land use cover change data was obtained by combining supervised classification and visual interpretation (Table 1). Land use data were obtained every 5 years from 2010 to 2020. NDVI data, with a resolution of 30 meters, was sourced from the National Ecological Science Data Center (<http://www.geodata.cn>). Net Primary Production (NPP) data was derived from the MOD17A3HGF dataset with a spatial resolution of 500 m. Landscape fragmentation and landscape disturbance indices were calculated using Fragstats. Terrain data, primarily from NASA (<https://doi.org/>), with a spatial resolution of 30 m, was used to process topographic relief and elevation data.

The habitat quality index was simulated using the Integrated Valuation of Ecosystem Services and Trade-offs (InVEST) model. Soil erosion data was calculated using the Revised Universal Soil Loss Equation (RUSLE). Population density data, with a resolution of 100 m, were sourced from the World Population Database (<https://hub.worldpop.org/>). GDP data, with a resolution of 250 m, was sourced from the Geographic Remote Sensing Ecological Network (www.gisrs.cn). Ecological sensitivity and human disturbance indices were calculated based on land use data. Meteorological data, with a resolution of 1 km, was sourced from the Geographic Resource Data Cloud (www.gscloud.cn).

To ensure spatial consistency of all data, it was processed by clipping, projection, and resampling to a spatial resolution of 30 m.

Methods

Description and extraction of ECC assessment factors

Amount of soil erosion. Soil erosion is a fundamental indicator of ecological quality and illustrates the ecological impact of human interactions⁴⁵. The RUSLE model is a basic tool for assessing soil erosion⁴⁶. Its formula is as

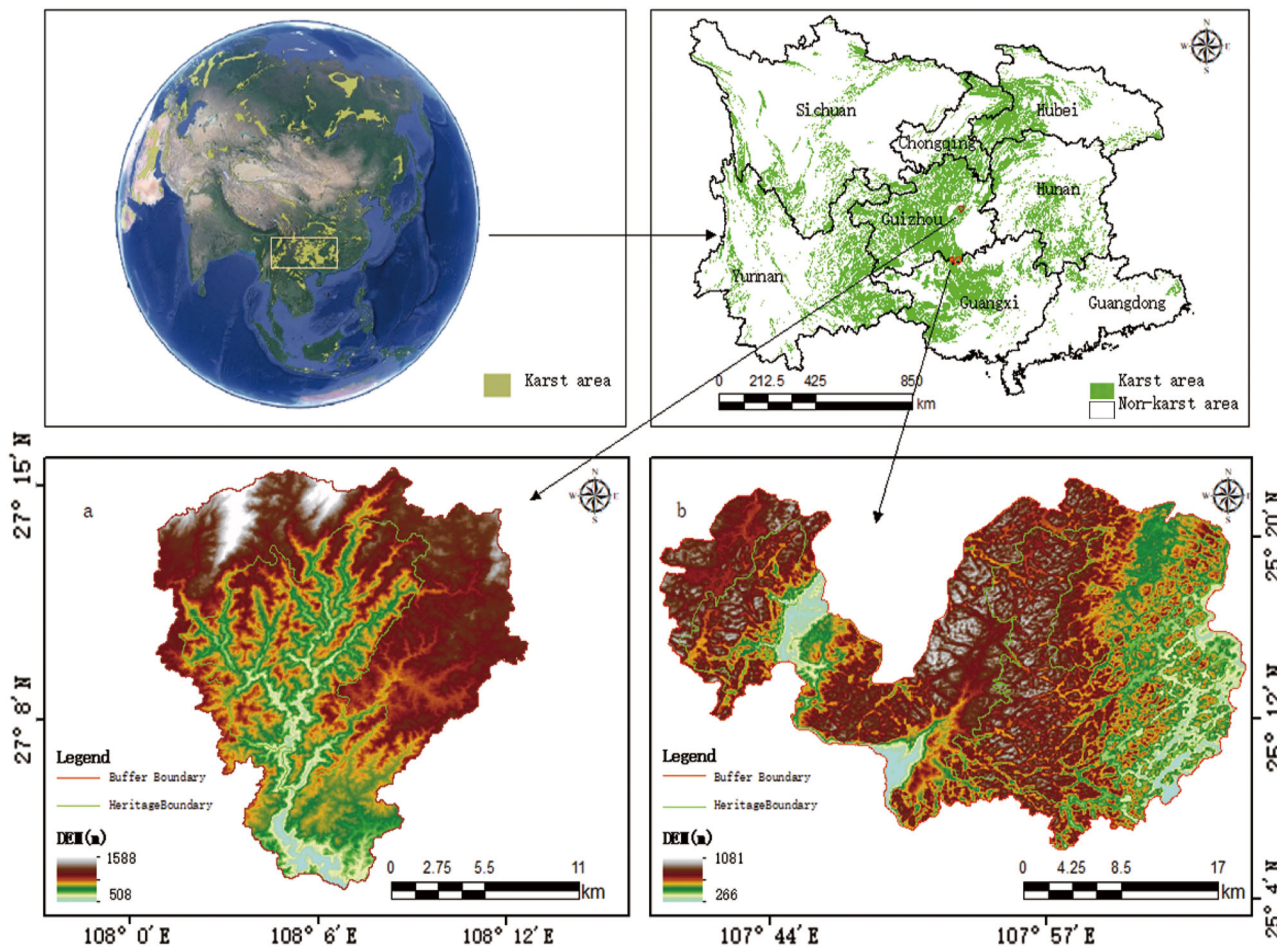


Fig. 1 | The location of Study area. a represents Shaping heritage site; b represents Libo-Huanjiang heritage site.

Table 1 | Data source and description

Data	Resolution	Unit	Particular year	Source
Land use types	30 m	-	2010/2015/2020	Resource and Environmental Science and Data Center (https://www.resdc.cn)
NPP	500 m	-	2010/2015/2020	NASA (https://www.nasa.gov)
GDP	250 m	-	2010/2015/2020	Geo-Remote Sensing Ecological Network (www.gisrs.cn)
Population data	100 m	-	2010/2015/2020	World Population Database (https://hub.worldpop.org/)
Terrain conditions	30 m	-	-	NASA (https://www.nasa.gov)
Temperature	1000 m	°C	2010/2015/2020	Geo-resource data cloud (www.gscloud.cn/)
NDVI	30 m	-	2010/2015/2020	National Ecological Science Data Center (http://www.geodata.cn)
Soil	1000 m	-	-	Harmonized World Soil Database (https://gaez.fao.org/)
Precipitation	1000 m	mm	2010/2015/2020	Geo-resource data cloud (www.gscloud.cn/)
Evaporation	1000 m	-	2010/2015/2020	Geo-resource data cloud (www.gscloud.cn/)

follows:

$$A = R \times K \times L \times S \times C \times P \quad (1)$$

Among them, A is the actual annual average soil erosion modulus; R is rainfall erosivity factor; K is soil erodibility factor; L and S are slope length and slope factor, dimensionless; C is the surface vegetation coverage and management factor, dimensionless; P is the factor of soil and water conservation measures, dimensionless.

Habitat quality index. Habitat quality index represents the self-regulation and self-sustaining ability of regional ecosystems. In this paper, the InVEST

model is used to evaluate the habitat quality index⁴⁷. The calculation method is shown in the formula:

$$Q_{xj} = H_j \left\{ 1 - \left(\frac{D^z_{xj}}{D^z_{xj} + K^z} \right) \right\} \quad (2)$$

In the formula, Q_{xj} is the habitat quality of patches in land use type j ; H_j is the habitat suitability of patches in land use type j ; D^z_{xj} is the threatened level of patches in land use type j , and z is a constant.

Landscape fragmentation and landscape disturbance index. Different landscape types play different roles in maintaining biodiversity, improving landscape structure, and promoting the overall function of the landscape. At the same time, they have different resistance to external disturbances. Landscape disturbance and landscape fragmentation represent the pressure of environmental damage. In this paper, the landscape disturbance index is constructed with reference to^{48,49}, and the formula is:

$$LDI_i = aC_i + bH_i + cF_i \quad (3)$$

Among them, a, b and c are the weights of landscape fragmentation, diversity index and fractal dimension, respectively, reflecting the influence of each index on the ecological environment represented by the landscape to varying degrees, in which $a + b + c = 1$; the weights of research results a, b and c in related fields are 0.5, 0.3 and 0.2; LDI_i is landscape disturbance index, C_i is landscape fragmentation, landscape fragmentation, H is diversity index, F_i is fractal dimension.

Other factors. Ecological sensitivity is an important indicator of regional ecosystem stability. According to related research, the ecological sensitivity evaluation results were calculated based on five factors: vegetation cover, elevation, slope, slope direction, and land use type⁵⁰. Land use intensity and development interference index reflect the degree of human exploitation of the ecological environment, and both factors are calculated based on land use data^{51,52}. Climate indicators are fundamental components of ecosystems, driving material cycles and energy flows within the system⁵³. Among them, temperature, precipitation, and evapotranspiration directly reflect regional climatic conditions, which have significant impacts on regional ecosystems, residents' lives and social production. Vegetation condition directly affects the structure and function of ecosystems^{54,55}. NDVI and NPP directly reflect the growth condition of regional vegetation and the quality of ecological environment⁵⁶. Topographic relief and elevation data directly or indirectly affect the regional ecological environment through microclimate differentiation. In addition, human activities also affect the ecological environment, such as population density and economic development index reflect the degree of exploitation of nature by human activities to a certain extent.

ECC assessment

Analytic Hierarchy Process. The Analytic Hierarchy Process (AHP) is a decision-making method that decomposes a problem into multiple levels of objectives, criteria, and alternatives, allowing for both qualitative and quantitative analysis⁵⁷. The specific steps of the AHP are as follows:

- (1) Use Yaahp10.5 software to build a hierarchical structure model, including the target layer, influencing factor layer, and index layer.
- (2) Set the impact indicators. The n indexes that affect the ECC are set as $y_1, y_2, y_3, \dots, y_n$.
- (3) Construct a comparison matrix. Starting from the second layer, use the comparison matrix and the 1–9 scale method to measure the importance of each pair of indicators. Experts in the field score the relative importance of each index, and the average values are calculated. The Delphi method is then used to obtain the comparison scale value for each index, forming the judgment matrix. Based on the judgment matrix, the relative importance of indicators at this level is compared in pairs. Matrix analysis allows for a clear understanding of the main influencing factors at this and the previous levels. The 1–9 scale method is used to evaluate the judgment matrix, as shown in Table 2.
- (4) Construct the judgment matrix. The importance of different indicators is scored according to Tables 2, 3, and the judgment matrix is constructed:

$$X = \begin{bmatrix} x_{1,1} & x_{1,2} & \dots & x_{1,n} \\ \vdots & \vdots & \ddots & \vdots \\ x_{n,1} & x_{n,2} & \dots & x_{n,n} \end{bmatrix} \quad (4)$$

- (5) Calculate the maximum eigenvalue and its corresponding eigenvector of matrix X:

$$\lambda_{\max} = \frac{1}{n} \times \sum_{i=1}^n \sum_{j=1}^n x_{i,j} \times \frac{\omega_j}{\omega_i} \quad (5)$$

- (6) Standardize the eigenvector^{58,59}. The λ_{\max} eigenvector, is calculated and normalized, $\omega = (\omega_1, \omega_2, \omega_3, \dots, \omega_n)$, and satisfies $\omega_n = \sum_{j=1}^n x_{i,j} / \sum_{j=1}^n \sum_{i=1}^n x_{i,j}$. Using the power method, the maximum eigenvalue of the matrix X and its corresponding eigenvector ω are calculated and standardized.

- (7) Calculate the consistency index. Consistency indicators:

$$CI = \lambda_{\max} - n/n - 1 \quad (6)$$

- (8) Consistency test. By looking up the table to analyze the n value, the CR value of the random index is obtained, and the CI/CR value is calculated. If the CI/CR value is less than or equal to 0.1, it indicates that the inconsistency of the matrix X is acceptable, that is, the hierarchical total ranking meets the requirements of the consistency test.

CRITIC weight method. The CRITIC weighting method, which determines weight through the correlation between indicators, is an objective weighting method. Its core principle is to comprehensively consider the indicators of contrast strength and conflict⁶⁰. The specific steps are as follows:

- (1) Data standardization:

Differences in the dimensions and attributes of the evaluation indicators need to be standardized. Based on their connotations, indicators are defined as positive or negative. Positive indicators have a positive impact on the corresponding aspects of ECC, while negative indicators have a negative impact.

Positive indicators:

$$Y_{ij} = x_j - x_{\min} / x_{\max} - x_{\min} \quad (7)$$

Negative indicators:

$$Y_{ij} = x_{\max} - x_j / x_{\max} - x_{\min} \quad (8)$$

In the formula: Y_{ij} represents the standard value of the i-year and j index, while X_{ij} is the original value of the I year and j index, and X_{\max} and X_{\min} represent the maximum and minimum values of the j-index, respectively.

- (2) Calculate the variability S_j within each index:

The index variability is expressed in the form of standard deviation. S_j represents the standard deviation of the jth index, where \bar{X}_j is the average value of the jth index.

$$\bar{X}_j = \frac{1}{m} \sum_{i=1}^m X_{ij} \quad (9)$$

$$S_j = \sqrt{\frac{1}{m-1} \sum_{i=1}^m (X_{ij} - \bar{X}_j)^2} \quad (10)$$

The CRITIC method uses the standard deviation to quantify the degree of variation in the values of each index. A larger standard deviation indicates a wider range of numerical variation for the index. Therefore, an index with a larger standard deviation has a stronger evaluation ability and should be assigned a higher weight.

Table 2 | Proportion scale table

Quantification	Compare results	Compare the situation
1	Equally important	Compared with the two factors, a and b are equally important.
3	Slightly important	Indicating that a is slightly more important than b compared to the two factors.
5	Obviously important	It shows that a is more important than b in the two factors.
7	Strongly important	It indicates that a is more important than b compared with the two factors.
9	Extremely important	It indicates that a is more important than b in comparing the two factors.
2, 4, 6, 8	The median value of two adjacent degrees	The comparison of the two indicators is between the above adjacent situations and needs to be compromised.

Table 3 | Evaluation index system of ECC

Criterion layer	Index	Index types	Comprehensive weight					
			Shibing HS			Libo-Huanjiang HS		
			2010	2015	2020	2010	2015	2020
Ecological resilience	NDVI	Positive	0.1343	0.1363	0.1357	0.1330	0.1312	0.1509
	NPP	Positive	0.0808	0.0812	0.0800	0.0811	0.0819	0.0820
	Elevation	Positive	0.0580	0.0592	0.0582	0.0631	0.0633	0.0638
	Temperature	Positive	0.0747	0.0749	0.0732	0.0780	0.0801	0.0818
	Precipitation	Positive	0.0839	0.0868	0.0850	0.0843	0.0864	0.0874
	Evaporation	Negative	0.0521	0.0543	0.0520	0.0576	0.0528	0.0532
	Topographic relief	Positive	0.0534	0.0548	0.0534	0.0502	0.0506	0.0510
Resources and environment supply capacity	Soil erosion amount	Negative	0.0259	0.0272	0.0363	0.0361	0.0329	0.0345
	Habitat quality index	Positive	0.0566	0.0578	0.0575	0.0640	0.0639	0.0609
	Ecological sensitivity	Negative	0.0375	0.0398	0.0387	0.0352	0.0327	0.0304
	Landscape fragmentation	Negative	0.0453	0.0399	0.0432	0.0382	0.0323	0.0393
	Landscape disturbance index	Negative	0.0609	0.0582	0.0597	0.0521	0.0512	0.0563
Ordination capability of social economy	Land use intensity	Negative	0.0864	0.0830	0.0814	0.0848	0.0878	0.0752
	Population density	Negative	0.0484	0.0471	0.0484	0.0506	0.0565	0.0548
	Economic development index	Negative	0.0286	0.0299	0.0288	0.0224	0.0228	0.0235
	Develop interference index	Negative	0.0733	0.0698	0.0686	0.0695	0.0737	0.0551

(3) Calculate the conflict R_j between indicators:

$$R_j = \sum_{j=1}^n (1 - r_{ij}) \quad (11)$$

The correlation coefficient measures the correlation between different indicators. If an index has a high correlation with other indicators, it indicates overlap in evaluation content, so the weight of such an index should be reduced.

(4) Calculate the amount of information C_j for each indicator:

$$C_j = S_j \sum_{j=1}^n (1 - r_{ij}) = S_j R_j \quad (12)$$

In the formula, the larger the C_j , the greater the role of the j th index in the entire evaluation index system, and more weight should be assigned to it.

(5) Calculate the weight of each index W_j :

$$W_j = \frac{C_j}{\sum_{j=1}^n C_j} \quad (13)$$

Comprehensive evaluation method and classification. ECC is a critical index for characterizing the current state of the regional ecological environment. A higher ECC indicates a better ecological environment. The ECC results are obtained by applying the weight of each parameter to the evaluation parameters and then summing the results⁶¹. To facilitate the comparison of multi-period ECC index, standardization is necessary.

$$ECC = \sum_{i=1}^n X_i \times W_i \quad (14)$$

$$I_{ECC,i} = \frac{ECC_i - ECC_{i,min}}{ECC_{i,max} - ECC_{i,min}} \quad (15)$$

ECC is the ECC, X_i is the standardized value of the parameter, W_i is the weight value of the parameter, $I_{ECC,i}$ is the standardized value of the ecosystem in the i year, and $ECC_{i,max}$ is the maximum value of the ECC index in the i year. $ECC_{i,min}$ is the minimum value of the ECC index in the i year.

Based on the natural geographical characteristics of Shbing and Libo-Huanjiang KWHS, and referencing the ECC and study area characteristics, the ECC is divided into five levels: weakest (0–0.2), weaker (0.2–0.4), medium (0.4–0.6), stronger (0.6–0.8), and strongest (0.8–1).

Analysis of spatial aggregation of ECC. In this study, the Getis-Ord G_i^* index is used to analyze the high/low spatial aggregation of ECC. The spatial distribution of cold and hot spots is calculated as follows⁶²:

$$G_i^* = \frac{\sum_{j=1}^n w_{i,j} x_j - \bar{X} \sum_{j=1}^n w_{i,j}}{\sqrt{\left[n \sum_{j=1}^n w_{i,j}^2 - \left(\sum_{j=1}^n w_{i,j} \right)^2 \right] / (n-1)}} \quad (16)$$

$$\bar{X} = \frac{1}{N} \sum_{j=1}^n x_j \sqrt{\left(\frac{1}{n} \sum_{j=1}^n x_j^2 - \bar{X}^2 \right)} \quad (17)$$

In the formula: n represents the total number of patches in the region, G_i^* is the output statistical Z score, x_j is the attribute value of the spatial unit j , and $w_{i,j}$ is the spatial weight between the adjacent spatial units and.

Analysis of ECC drivers. Geodetector are powerful tools for detecting spatial heterogeneity and identifying the main drivers of spatial heterogeneity, including factor detection, interaction detection, ecological detection and risk area detection⁶³. This paper uses a factor test to explore the specific effects of the 16 drivers on ECC (i.e., explanatory power q -values), and an interaction test to confirm the extent to which any two drivers interact to contribute to ECC. The specific steps are as follows:

- (1) Factor detector is mainly used to measure the spatial differentiation of ECC Y and the degree of interpretation of different influencing factors X . The calculation formula is:

$$q = 1 - \frac{\sum_{h=1}^L n_h \delta_h^2}{n \delta^2} = 1 - \frac{SSW}{SST} \quad (18)$$

$$SSW = \sum_{h=1}^L n_h \delta_h^2 \quad SST = \sum_{h=1}^L n \delta^2 \quad (19)$$

In the formula, q is the factor explanatory power, $h = 1, 2, \dots, L$ is the number of classifications; n_h and n are the number of sample units in layer h and the whole region, respectively. δ_h^2 and δ^2 are the variance of layer h and the whole region, respectively. SSW is the sum of the intra-layer variance, and SST is the sum of the total variance of the whole region. The value range of q is $[0,1]$. The larger the q value is, the stronger the explanatory power of the impact factor to the spatial differentiation of ECC is.

- (2) Interaction detection is used to identify the interaction between different influencing factors, that is, to assess whether the combined effects of X_1 and X_2 will increase or decrease the explanatory power of ECC or the effects of these factors on the spatial distribution of ECC are independent of each other. The interaction mainly identifies the influence of the interaction between the two influencing factors on the change of ECC by calculating the sum of the q values of the two factors and the q value of the combination of the two influencing factors. Where $q(x \cap y)$ denotes the interaction between x and y , $\text{Min}(q(x), q(y))$ denotes the minimum value between $q(x)$ and $q(y)$, $\text{Max}(q(x), q(y))$ denotes the maximum value between $q(x)$ and $q(y)$, and $q(x) + q(y)$ denotes the sum of $q(x)$ and $q(y)$.

Results

Construction and weighting of ECC indicator system

The ECC of KWHS is affected by a combination of factors. And considering the representativeness and availability of the influencing factors, this paper screened 16 factors from three aspects, namely, ecological resilience, resource and environmental supply capacity, and socio-economic coordination capacity, and obtained their weights according to the weight

calculation method. The influence factors are represented by X , i.e., NDVI (X1), NPP (X2), elevation (X3), temperature (X4), precipitation (X5), evaporation (X6), topographic relief (X7), soil erosion (X8), habitat quality index (X9), ecological sensitivity (X10), landscape fragmentation (X11), landscape disturbance index (X12), land use intensity (X13), population density index (X14), economic development index (X15) and development disturbance index (X16) (Fig. 2 and Table 3).

Spatial variation characteristics of ECC

The spatial differentiation of ECC in the KWHS is pronounced, presenting an overall spatial layout of high core area and low buffer zones (Fig. 3), which is closely related to the natural and socio-economic environment of the KWHS.

From 2010 to 2020, the weakest and weaker ECC zones of Shbing HS have changed little, with a slow growth trend over the decade, and are mainly located in the buffer zone. The zones with medium, stronger and strongest ECC are mainly distributed in the core zone and the buffer zone with less human activities, in which the medium ECC zone shows a 'V'-shaped trend of change, with a slow overall change, while the stronger and strongest ECC zone show significant changes. It is worth noting that from 2015 to 2020, the core area of Shbing HS is mainly at the medium ECC level.

From 2010 to 2020, the zones with weakest and weaker ECC in the Libo-Huanjiang HS change less, showing an inverted 'V' trend, and are mainly distributed in the buffer zone, with only sporadic distribution in the core zone. On the other hand, the area of medium, stronger and strongest ECC zones changes significantly, of which medium ECC zones are mainly distributed in the buffer zone and the transition area between the buffer zone and the core zone, stronger ECC zones have larger areas and are mainly distributed in the buffer zone and part of the core zone, and the strongest ECC zones are more centrally distributed, mainly in the southeastern part of the site and near the watershed of the buffer zone. It is worth noting that the ECC of the core area of the Libo-Huanjiang HS has slightly decreased from 2015 to 2020.

Temporal variation characteristics of ECC

To further clarify the spatial distribution of ECC changes in the KWHS, this study utilized ArcGIS 10.6 software to analyze ECC results and obtained dynamic monitoring maps for the periods 2010–2015, 2015–2020, and 2010–2020 (Figs. 4–5).

In 2010–2015, the ECC of Shbing HS is relatively stable, the area of medium, stronger and strongest ECC area accounts for 96.32% of the total area of the HS, the area of weakest ECC area is slightly larger than the area of weaker ECC area, mainly scattered in the buffer zone and the middle of the core area. 2015–2020, the area of medium, stronger and strongest ECC area shows a trend of shrinkage, only accounting for 70.19% of the total area of the of Shbing HS, while the area of the weaker ECC area increases significantly. 2010–2020 the area of the strongest ECC area of the Shbing HS is drastically reduced, and the area of the medium, stronger and strongest ECC area is only 168.46 km² accounting for 59.66% of the total area of the HS. Overall, the ecological and environmental conditions of Shbing HS regress from 2010 to 2020.

In 2010–2015, the ECC of Libo-Huanjiang HS is comparatively good, with 92.49% of the total area of the site in the medium, stronger, and strongest ECC zones, while the area of the weakest ECC zone increases slightly, mainly in the vicinity of populated settlements in the buffer zone and in the core zone where anthropogenic modifications are obvious. In 2015–2020, the area of medium ECC area increases significantly, reaching 141.95 km², while the area of strongest ECC area is opposite, and the area of stronger ECC area remains stable, which is mainly manifested in the local degradation of the core area with high ECC to medium ECC area. 2010–2020, the area of low ECC area gradually expands, while the area of high ECC area locally degrades to medium ECC area. In general, the overall degradation of the ECC in 2010–2020 is obvious.

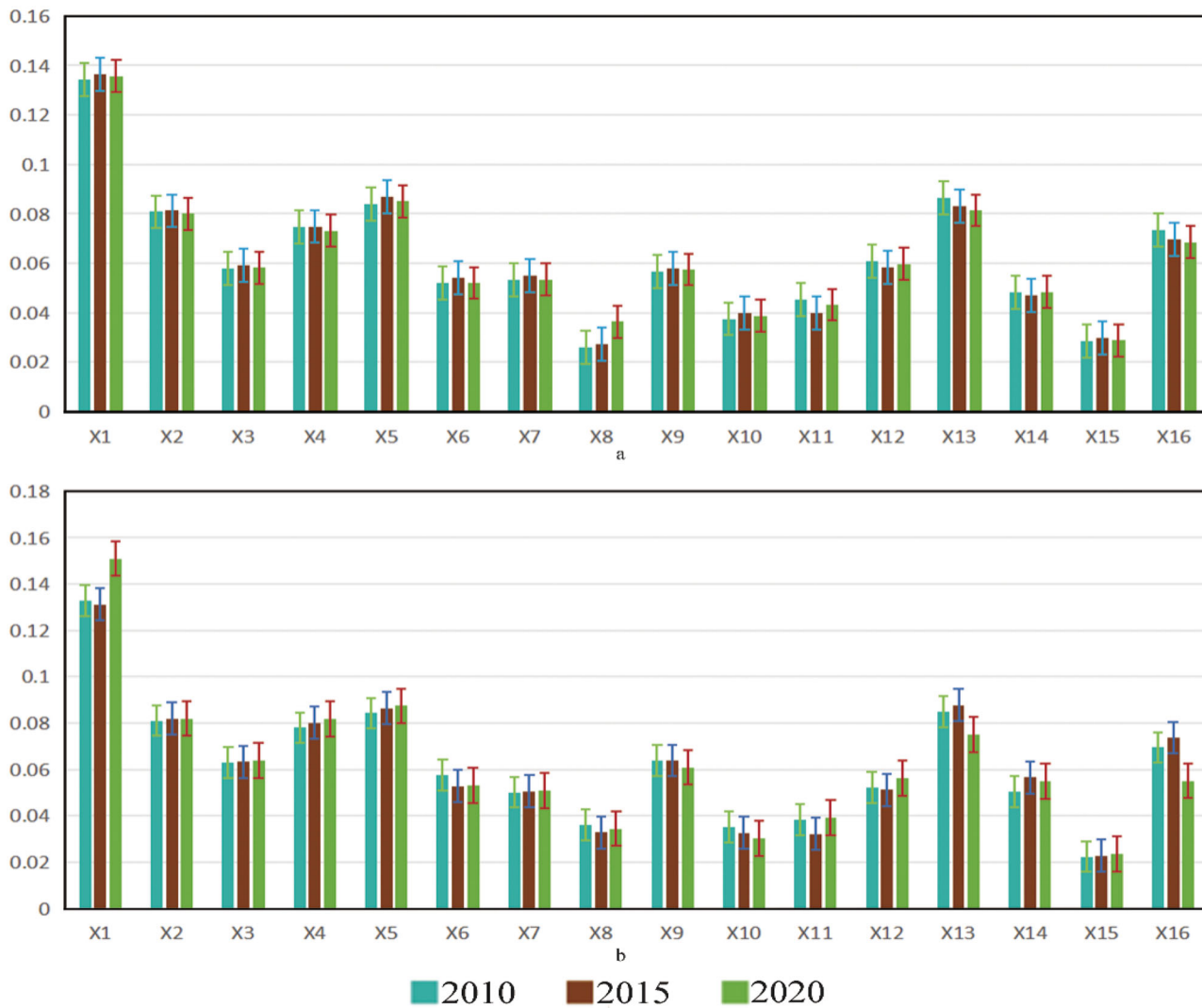


Fig. 2 | Influence factor weight ranking. a represents Shiping heritage site; b represents Libo-Huanjiang heritage site.

Spatial aggregation characteristics of ECC

The ECC of the KWHS for the years 2010, 2015, and 2020 were calculated, and the average values were derived using a 300×300 grid. Subsequently, a spatial cold and hot spot cluster analysis was performed, followed by a significance test. The results are presented in Fig. 6. Hot spot clusters represent areas with high ECC values, while cold spot clusters represent areas with low ECC values.

The hotspot gathering area of Shiping HS is mainly distributed in the core area, the western transition zone between the core area and the buffer zone, and the northern part of the area where human interference is weak (99% confidence level), which is dominated by the forest ecosystem, with a more complete system structure, less anthropogenic interference, and a high ECC of the ecosystem. The cold spot aggregation area is mainly distributed in the anthropogenic activity area of the buffer zone (confidence level 95–99%), where the intensity of anthropogenic interference is also relatively high, the system structure is simple, and the vegetation cover is poorer than that of the core area, so the ECC is lower. The ECC in 2015 was the best within the decade.

The hotspot aggregation area of Libo-Huanjiang HS is mainly distributed in the primitive forest area in the southeast of the site, and there are also sporadic distributions in the central part of the buffer zone (confidence level 99%). These areas are free of interference from human activities, have a warm climate, abundant precipitation, and have an intact ecosystem

structure, rich biodiversity, and a high level of ecological resilience, and thus have a high ECC of the ecosystem. Cold spot aggregation areas are mainly distributed in anthropogenic activity areas in the buffer zone, the transition zone between the core zone and the buffer zone, and local areas in the core zone (confidence level 95–99%), which have higher exposure to human activities, have lower vegetation cover than the primary forest area, and are vulnerable to global climate change, and thus have a lower ECC. The ECC in 2010 was the best in the decade.

Obstacle factor diagnosis of ECC

Single factor detection of ECC. The main influencing factors of the ECC of the KWHS were analyses from the perspective of natural and social factors, and the results are shown in Fig. 7. The factors with the strongest influence on the spatial differentiation of the ECC of the Shiping HS in 2010 were the land-use intensity and the economic development index, respectively, and the development interference index and the land-use intensity in 2015, and the development interference index and the habitat quality index in 2020. The explanatory power of the above factors on ECC is greater than 0.61, while the explanatory power of natural factors such as NPP, temperature, and soil erosion is smaller, indicating that the ecological environment in this area is more strongly affected by human interference.

The dominant factors causing spatial differentiation in ECC of Libo-Huanjiang HS from 2010 to 2020 are ecological sensitivity and habitat

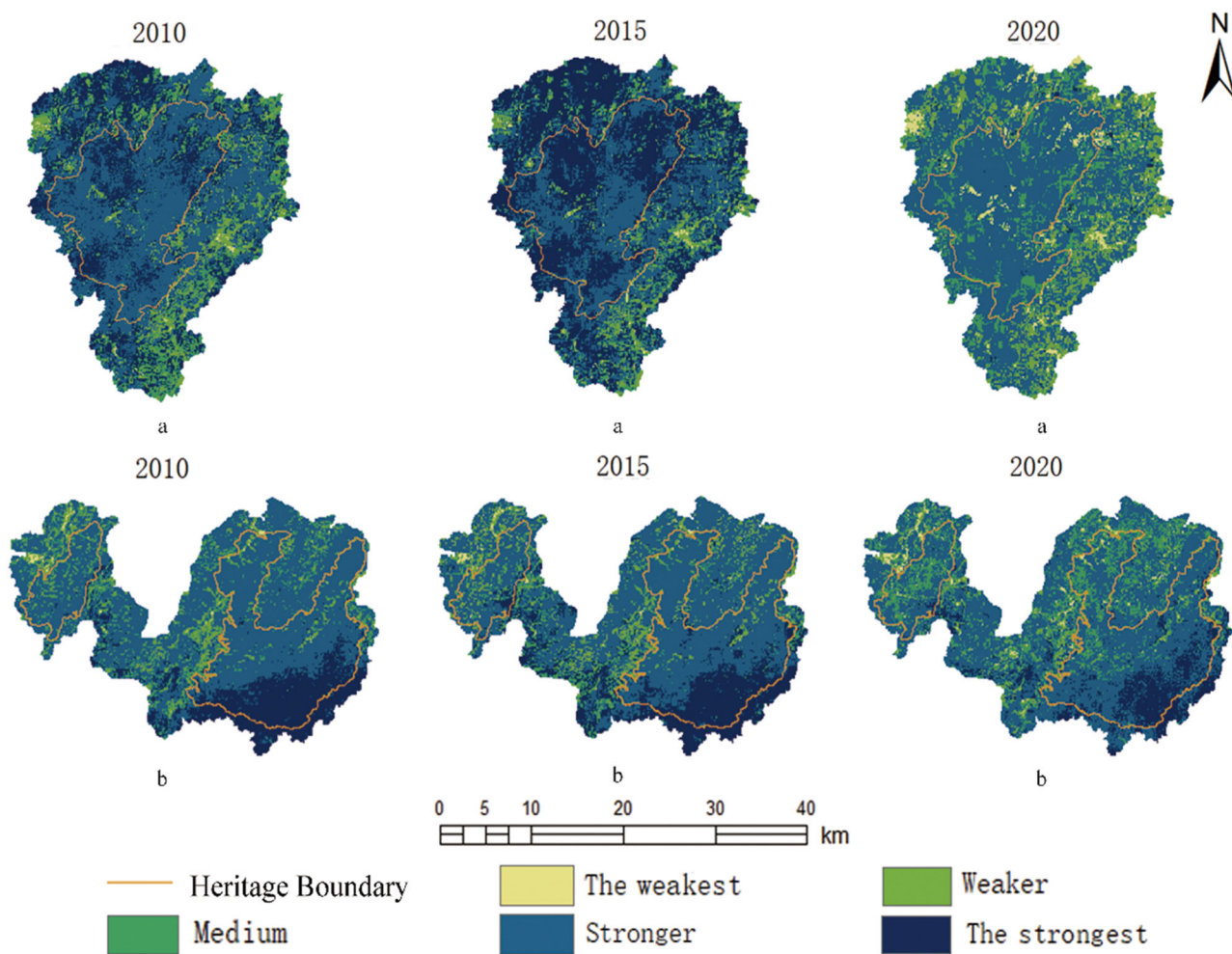


Fig. 3 | Spatial distribution of ECC from 2010 to 2020. a represents Shibing heritage site; **b** represents Libo-Huanjiang heritage site.

quality index, both of which have an explanatory power of more than 0.38 for ECC, followed by land-use intensity and landscape disturbance index, and natural factors such as elevation, evaporation, and amount of soil erosion have less explanatory power, indicating that the ecosystems of the Libo-Huanjiang HS are more complete and more strongly driven by natural factors.

Interactive detection of ECC factors. Factor interaction test can further analyses the effect of the interaction between different factors on the ECC, the results are shown in Fig. 8. 2010–2015, the stronger interaction of Shibing HS on the ECC is the land use intensity \cap NDVI, the economic development index \cap NDVI, and their explanatory power is more than 0.71. Secondly, the land use intensity, the development interference index has a strong interaction with other factors. The interactions with stronger explanatory power in 2020 were development disturbance index \cap NPP, land use intensity \cap development disturbance index and, landscape disturbance index \cap development disturbance index, with explanatory powers of 0.8042, 0.8039, and 0.8029, respectively, and both habitat quality index and development disturbance index had strong interactions with other factors, indicating that anthropogenic activities have always been an important factor influencing the ecosystem's development, indicating that anthropogenic activities have always been an important factor affecting the stability of the ecosystem.

In 2010, the interactions with higher explanatory power for ECC at Libo-Huanjiang HS were habitat quality index \cap ecological sensitivity, land use intensity \cap ecological sensitivity, with explanatory powers of 0.6297 and

0.5574, respectively. 2015 was the same as that of 2010, followed by stronger interactions between the habitat quality index, ecological sensitivity and other factors. The interactions with higher explanatory power for ECC in 2020 were habitat quality index \cap NDVI, ecological sensitivity \cap habitat quality index, and the interactions between other factors of land use intensity were significantly larger than those in 2010 and 2015. Overall, the interactions among multiple factors significantly enhanced the spatial variability of ECC.

Discussions

Spatial and temporal characteristics of ECC in KWHs

2010–2020, Shibing HS ECC overall degradation evolution trend, of which in 2010 the stronger ECC area dominated, 2015 strongest ECC area is the largest, 2020 degradation to the stronger ECC area is dominated. The main reason is that in 2010–2015 Shibing HS vegetation coverage, complex landscape structure and ecological functions, and slow economic development, tourism development is immature, the exploitation rate of nature and lower. Due to the 'WH' brand effect, from 2015 to 2020 Shibing HS tourism development is becoming more mature, the level of ecological environment development and utilization increased^{64–66}.

From 2010 to 2020, the ECC of Libo-Huanjiang HS showed an overall degradation trend, in which the ECC status was the worst in 2020, which showed that the strongest ECC area was degraded to a stronger ECC area, and the medium ECC area within the core area was expanded. The main reason is that the tourism development of Libo-Huanjiang HS is earlier, the tourism infrastructure is mature, the interference of human activities on the

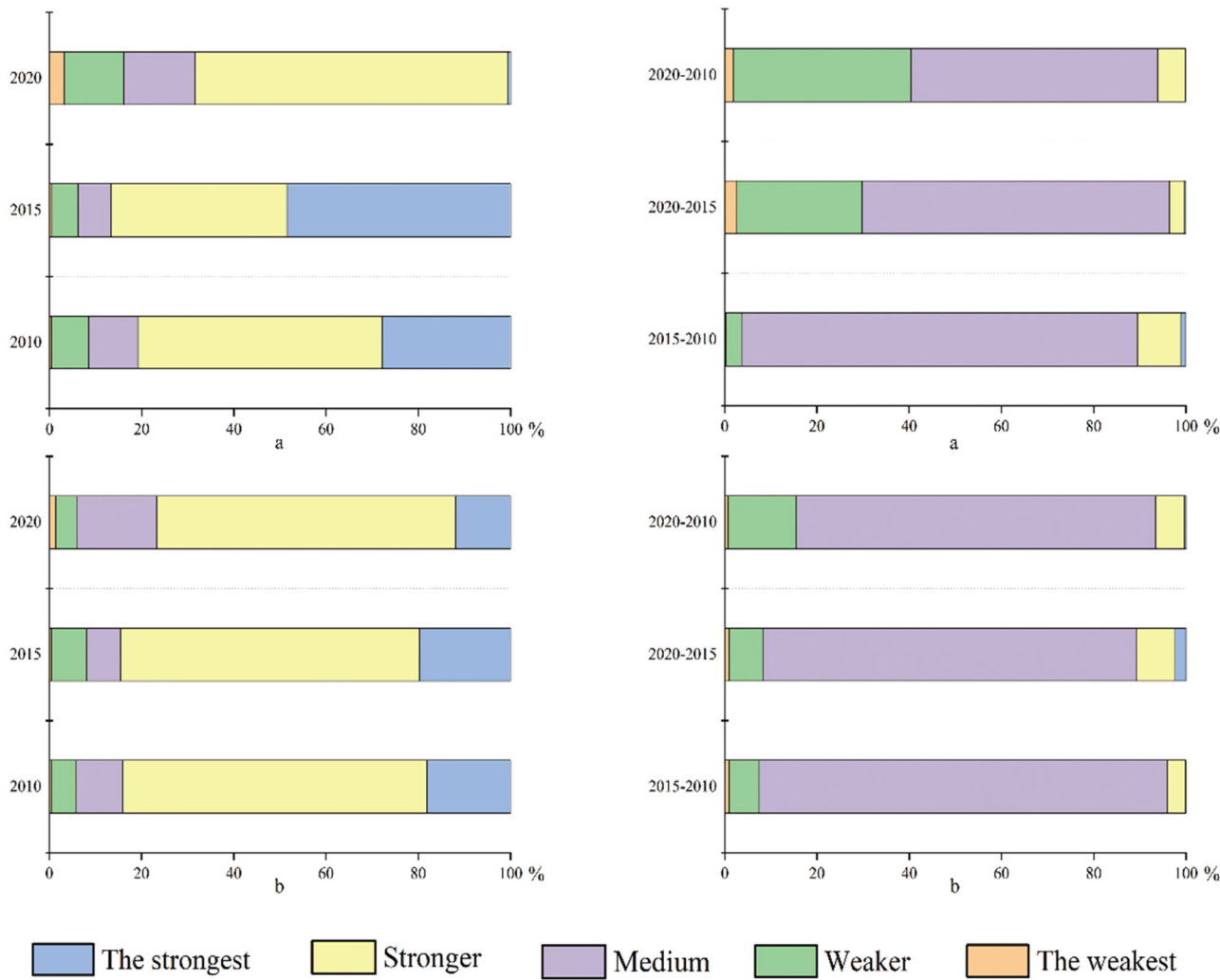


Fig. 4 | The proportion of different ECC area. a represents Shiping heritage site; b represents Libo-Huanjiang heritage site.

natural environment is enhanced, and its ecological environment is increasingly fragile^{43,67}. Overall, the ECC status of Libo-Huanjiang HS is better than that of Shiping HS from 2010 to 2020, and the degradation rate of ECC of Shiping HS is more obvious than that of Libo-Huanjiang HS.

ECC drivers for KWHS

Natural attributes and anthropogenic factors affect the spatial and temporal changes of regional ECC⁶⁸. This study found that the ECC of the KWHS was correlated with the habitat quality index, NDVI and ecological sensitivity factors. It reveals that natural factors are potential elements affecting regional ecological stability. Among the driving mechanisms of ecological risk in Bayinbuluk World HS in Xinjiang, landscape factors and natural environment factors are stronger drivers of ecological risk⁶⁹. In addition, land use intensity, development interference index and population density have strong correlation with ECC. The impacts caused by anthropogenic activities on regional ecological stability are rapid and strong. Natural HS can be ecologically restored to a certain extent under slow economic development⁷⁰. While agricultural production and tourism economic activities have negative ecological effects on KWHS, population density, tourism factors and woodland conservation have significant correlation with ecological vulnerability⁷¹.

In summary, the direction of sustainable development of the KWHS is indeed crucial in the context of increasing environmental problems. As the site is located in the southwest inland plateau with fragile ecological fundamentals, how to find a balance between community economic

development and heritage ecological protection has become a central issue in guiding the development of the KWHS.

Suggestions on ecological protection and management of KWHS

The South China KWHS is an exemplary karst landform and natural landscape, possessing significant aesthetic and tourism value⁷²⁻⁷⁴. It is significantly affected by the vulnerability of the karst environment and human activities, resulting in considerable ecological damage and numerous environmental problems. The uniqueness, vulnerability, and complexity of the KWHS ecological environment highlight the need for^{75,76}. To achieve stable and sustainable development of KWHS, it is crucial to address the close relationship between ecological environment protection and socio-economic development, particularly tourism economic development^{77,78}.

- (1) Insist on following the principles of sustainable development, community participation in publicity and education, and local residents as key factors in WH conservation and sustainable development⁷⁹.
- (2) Adhere to the development of ecotourism without damaging the health of the ecosystem, and encourage community participation in ecotourism activities⁸⁰. Increase pollution control in the upper reaches of the study area and adjacent areas, reduce the direct entry of tourism pollutants into natural areas, and take protective measures such as wastewater interception and treatment, river cleaning, and ongoing maintenance and monitoring⁸¹.

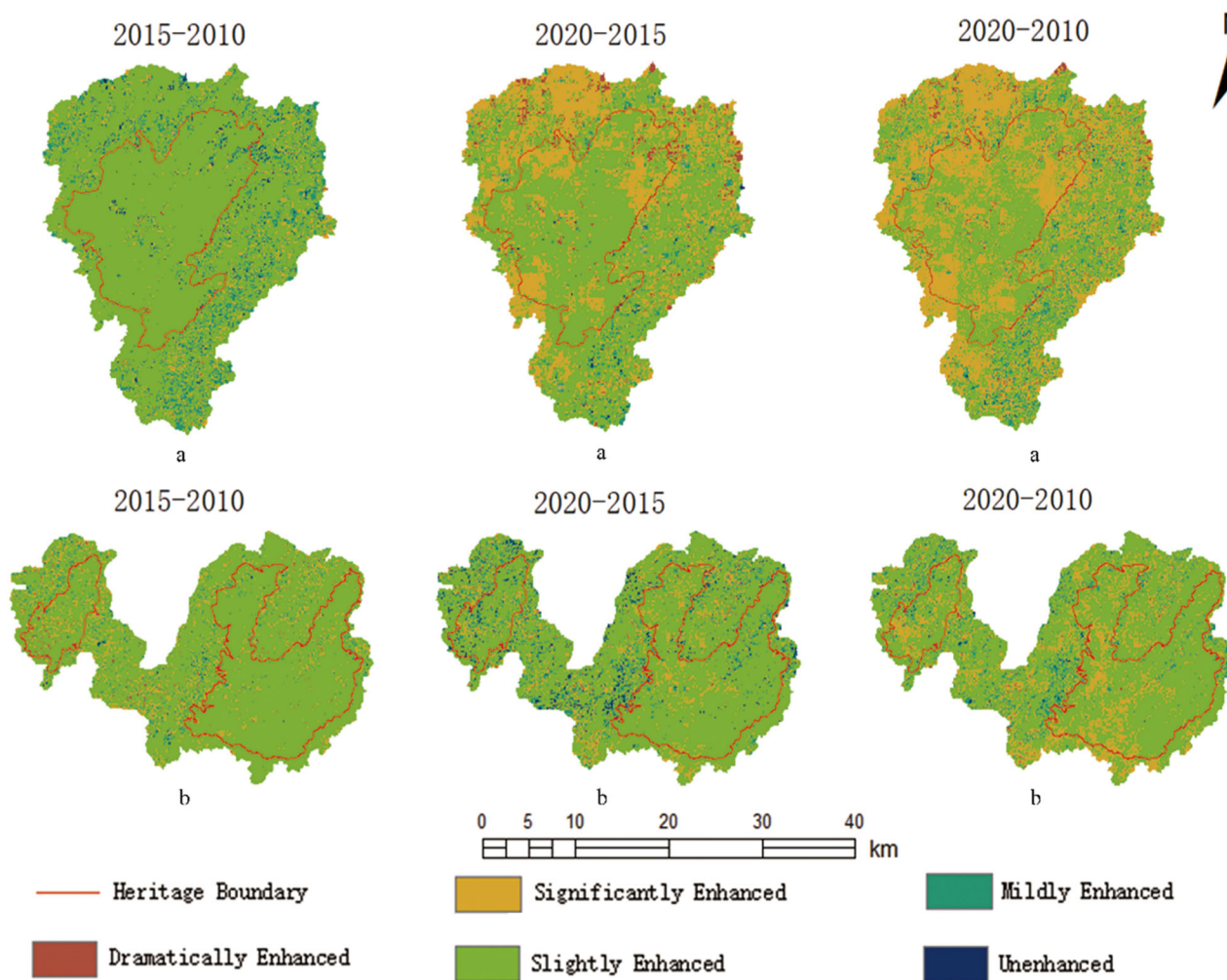


Fig. 5 | Time evolution characteristics of ECC. a represents Shbing heritage site; b represents Libo-Huanjiang heritage site.

(3) Enhance the environmental awareness of the main bodies related to tourism activities, multi-level units of government joint prevention, control and supervision to improve the ecological environment and maintain ecological stability. The sustainable development of WH tourism is the key to coordinating the relationship between heritage protection and utilization⁸².

To sum up, enhancing ecological security from multiple perspectives, such as increasing people's participation, encouraging the development of eco-tourism, as well as enhancing the environmental protection awareness of relevant subjects by the joint government, is an important way to enhance the ECC, and an important ecological foundation for the promotion of local economic development.

Limitations and future directions

This study is based on the evaluation of ECC by a combination of RS/GIS technology. However, on the one hand, due to the special positioning of the KWHS, limited socio-economic data about human activities can be collected. Therefore, the indicator system is constructed more mainly based on the natural environment elements. On the other hand, in the identification of impact factors, no clear indicator system has been found at home and abroad for reference, which may still be subjective according to the specific reality of the research object and the operability of each method, and may not completely and accurately reflect the ECC of the study area. To sum up, it is a difficult problem to construct the ECC

indicator system in a scientific and reasonable way⁸³. Therefore, it is necessary to further explore the future development trend of the ECC of the KWHS, with a view to providing reference for its future construction and development.

Conclusions

In this study, the spatial and temporal distribution of ECC of Shbing and Libo-Huanjiang HS among the KWHS in South China was analyzed, and the spatial aggregation characteristics and the driving factors of ECC were found during the period of 2010–2020. The conclusions are as follows:

- (1) Spatially, the ECC of the core areas of the two HS is significantly greater than that of the buffer zones, and the ECC of the buffer zones with no human disturbance is greater than that of the buffer zones with strong human activities.
- (2) The changes of ECC of the two HS are similar in time, and both of them show a degradation trend. Among them, the degradation rate of ECC in Shbing HS is significantly greater than that in Libo - Huanjiang HS.
- (3) The ECC of the two HS has strong spatial agglomeration and obvious spatial differentiation. The core area is the hotspot aggregation area, and the buffer area is the cold spot aggregation area.
- (4) The dynamic change of the ECC of the KWHS is the result of a combination of internal and external factors. The main driving factor of the ECC of Shbing HS is the natural environment factor, while the main driving factor of the ECC of Libo - Huanjiang HS is the socio-economic factors.

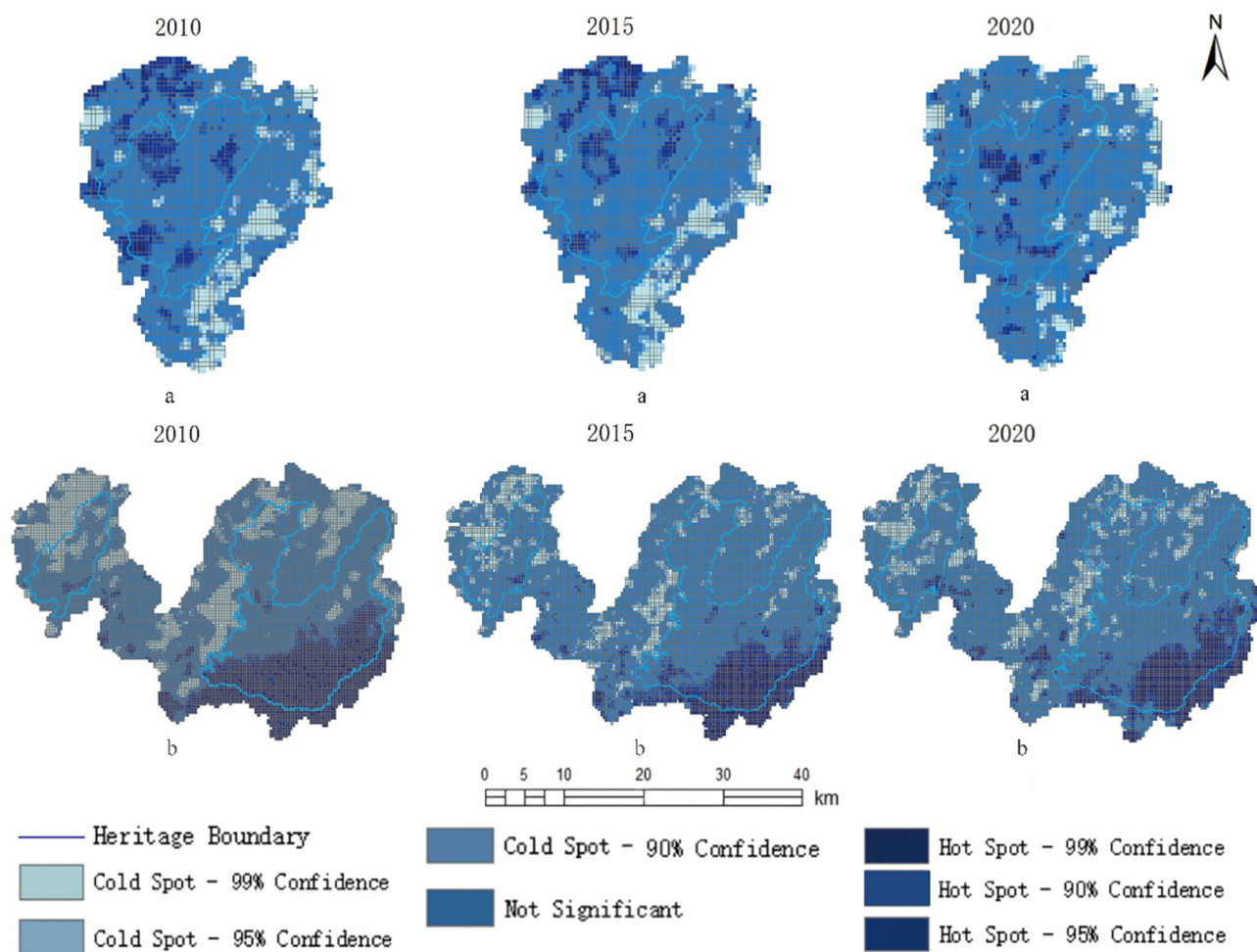


Fig. 6 | Spatio-temporal pattern characteristics of spatial cold and hot spots of ECC. a represents Shbing heritage site; b represents Libo-Huanjiang heritage site.

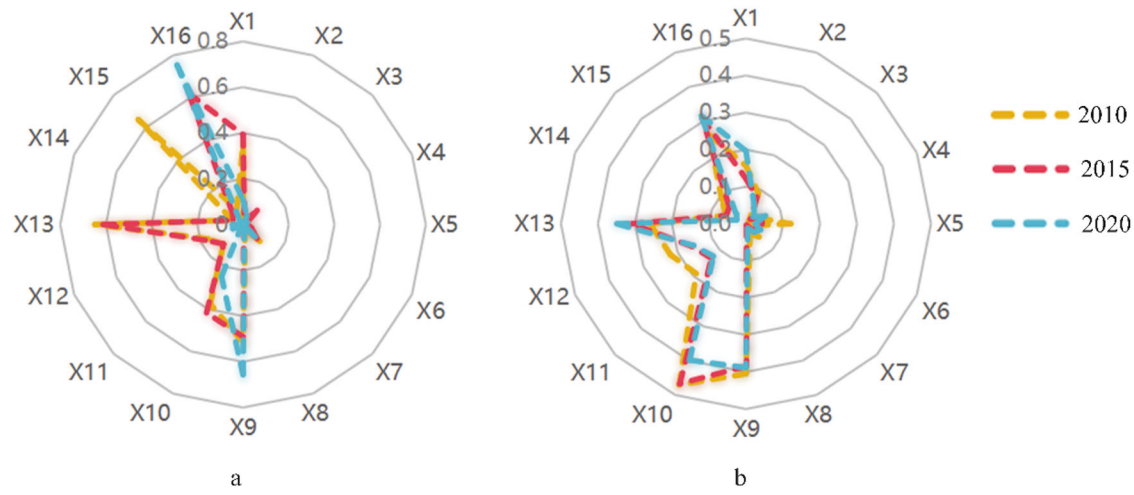


Fig. 7 | Detection of influencing factors of ECC. a represents Shbing heritage site; b represents Libo-Huanjiang heritage site.

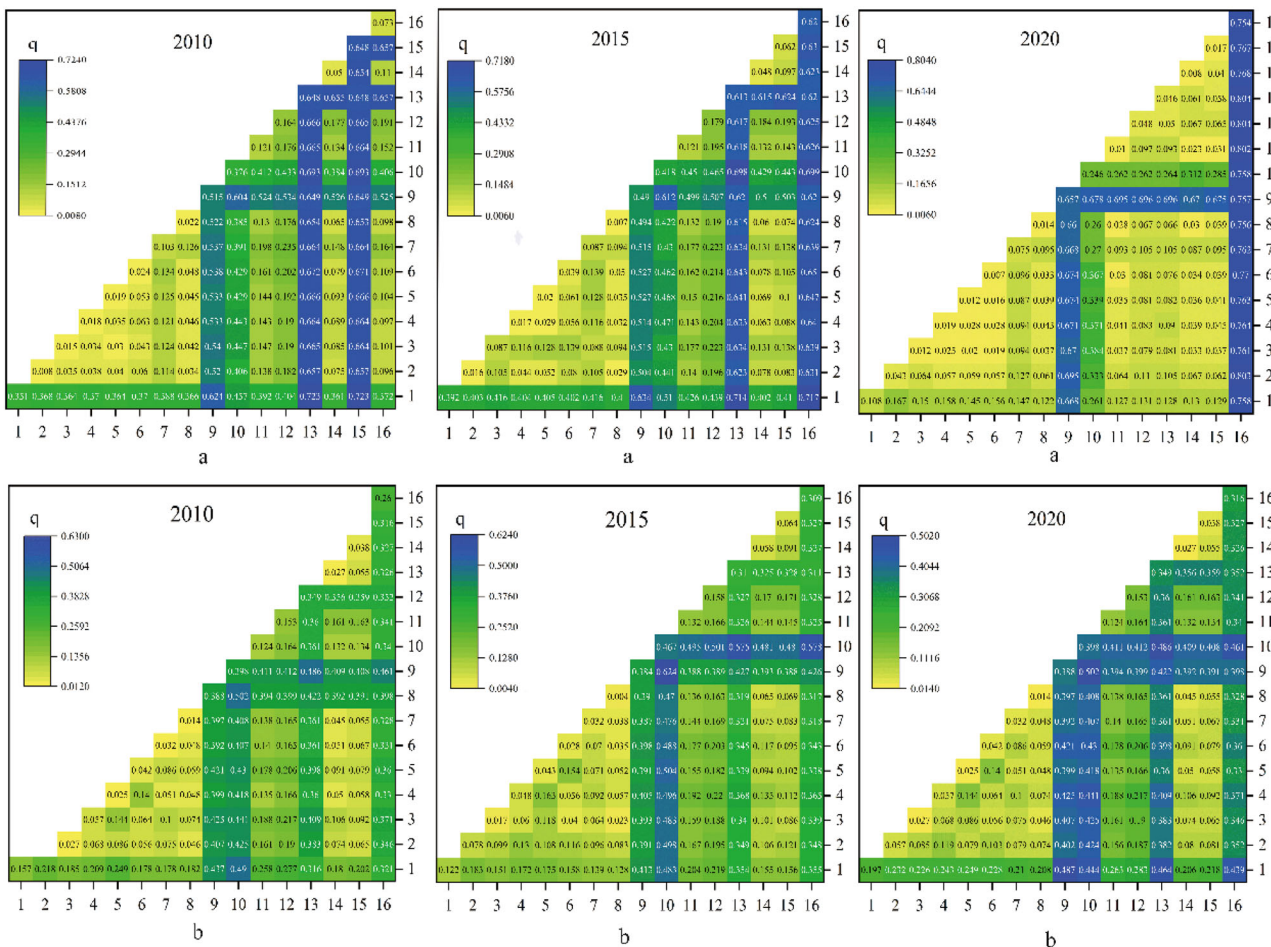


Fig. 8 | Interactive detection of ECC factors. a represents Shiping heritage site; b represents Libo-Huanjiang heritage site.

Data availability

Data are available from the authors upon requests.

Abbreviations

ECC	Ecosystem carrying capacity
KWHS	Karst world heritage site
HS	Heritage Site
WH	World heritage
NPP	Net Primary Production
AHP	Analytic Hierarchy Process

Received: 15 July 2024; Accepted: 25 November 2024;

Published online: 22 February 2025

References

1. Kowe, P., Mutanga, O., Odindi, J. & Dube, T. A quantitative framework for analysing long term spatial clustering and vegetation fragmentation in an urban landscape using multi-temporal landsat data. *Int. J. Appl. Earth Observ. Geoinf.* **88**, 102057 (2020).
2. Galli, A., Halle, M. & Grunewald, N. Physical limits to resource access and utilisation and their economic implications in Mediterranean economies. *Environ. Sci. Policy* **51**, 125–136 (2015).
3. Peng, J., Zhao, H. J., Liu, Y. X. & Du, Y. Y. Construction of regional water security pattern: research progress and conceptual framework. *Ecology* **36**, 3137–3145 (2016).
4. Qu, X. Q. et al. Research progress on evaluation methods of ecological carrying capacity. *J. Meteorol. Environ.* **35**, 113–119 (2019).
5. Park R. E. & Burgess E. W. *Introduction to the Science of Sociology* (University of Chicago Press, 1924).
6. Yue D. RS & GIS-based spatial analysis on ecological carrying capacity pattern of Northwest China: Does supply meet demand? *Quat. Int.* **551**, 279–280 (2012).
7. Odum E. P. & Barrett G. W. *Fundamentals of ecology* (Saunders, 1971).
8. Odum E. P. *Ecology and our endangered life-support systems* (Oxford University Press, 1993).
9. Godschalk, D. R. & Parker, F. H. Carrying capacity: a key to environmental planning? *J. Soil Water Conserv.* **30**, 160–165 (1975).
10. Harris, J. M. & Kennedy, S. Carrying capacity in agriculture: global and regional issues. *Ecol. Econ.* **29**, 443–461 (1999).
11. Wang, Y., Peng, B., Wei, G. & Elahi, E. Comprehensive evaluation and spatial difference analysis of regional ecological carrying capacity: a case study of the Yangtze River urban agglomeration. *Int. J. Environ. Res. Public Health* **16**, 3499 (2019).
12. Chen, J. Y., Huang, X. H., Ye, J., Wen, Z. L. & CF, Z. Spatial and temporal variation and driving factors of ecological carrying capacity in the Pan-Pearl River Basin, China. *Ecol. Indic.* **151**, 110318 (2023).
13. Yang X. Z. *Environmental management* (Higher Education Press, 1990).
14. Chen, Y., Tian, W. T., Zhou, Q. & Shi, T. Spatiotemporal and driving forces of ecological carrying capacity for high-quality development of 286 cities in China. *J. Clean. Prod.* **293**, 126186 (2021).
15. Shan, S. Y., Xu, H. J., Qi, X. L., Chen, T. & Wang, X. D. Evaluation and prediction of ecological carrying capacity in the Qilian Mountain National Park, China. *J. Environ. Manag.* **339**, 117856 (2023).

16. Shi, Y. Q., Liu, Z., Geng, W. & Li, W. Implementation of early warning method for ecological environment carrying capacity of Tianchi scenic spot in Changbai Mountain. *Ekoloji Dergisi*. **107**, 3623 (2019).
17. Zhao, Q. S. et al. Analysing ecological carrying capacity of bivalve aquaculture within the Yellow River Estuary ecoregion through mass-balance modelling. *Aquac. Environ. Interact.* **14**, 147–161 (2022).
18. Peng, T., Deng, H. W., Lin, Y. & Jin, Z. Assessment on water resources carrying capacity in karst areas by using an innovative DPESBRM concept model and cloud model. *Sci. Total Environ.* **767**, 144353 (2021).
19. Shi, T. T. et al. Dynamic evolution of the ecological carrying capacity of poverty-stricken karst counties based on ecological footprints: a case study in Northwestern Guangxi, China. *Int. J. Environ. Res. Public Health* **17**, 991 (2020).
20. Zhang, Z., Hu, B. Q., Jiang, W. G. & Qiu, H. H. Construction of ecological security pattern based on ecological carrying capacity assessment 1990–2040: a case study of the Southwest Guangxi Karst-Beibu Gulf. *Ecol. Model.* **479**, 110322 (2023).
21. Wang, B., He, W. J., Min, A., Xue, F. & Ramsey, T. S. Natural capital accounting of land resources based on ecological footprint and ecosystem services value. *Sci. Total Environ.* **914**, 170051 (2024).
22. Wu, T. X., Sang, S., Wang, S. D., Yang, Y. Y. & Li, M. Y. Remote sensing assessment and spatiotemporal variations analysis of ecological carrying capacity in the Aral Sea Basin. *Sci. Total Environ.* **735**, 139562 (2020).
23. Wu, X. L. & Hu, F. Analysis of ecological carrying capacity using a fuzzy comprehensive evaluation method. *Ecol. Indic.* **113**, 106243 (2020).
24. Wei, Z. Q., Ji, D. D. & Yang, L. Comprehensive evaluation of water resources carrying capacity in Henan Province based on entropy weight TOPSIS—coupling coordination—obstacle model. *Environ. Sci. Pollut. Res.* **30**, 115820–115838 (2023).
25. Qiu, H. H., Hu, B. Q. & Zhang, Z. Impacts of land use change on ecosystem service value based on SDGs report—Taking Guangxi as an example. *Ecol. Indic.* **133**, 108366 (2021).
26. Zhang, X. Y., Lu, L. Y., Yu, H., Zhang, X. & Li, D. H. Multi-scenario simulation of the impact of land use change on ecosystem service value in the Qinghai-Tibet Plateau. *J. Ecol.* **40**, 887–898 (2021).
27. Che, Y. J. et al. Spatio-temporal pattern of world heritage and its accessibility assessment in China. *Sustainability* **14**, 3033 (2022).
28. Yang, X. S., Mu, D. J., Hu, M. J., Xiao, S. Z. & Meng, J. N. Establishment of the management effectiveness assessment system of world natural heritage and empirical analysis—a case study of Fan jingshan. *Herit. Sci.* **11**, 124 (2023).
29. Stott, P. H. The world heritage convention and the national park service: the first two decades, 1972–1992. *George Wright Soc.* **29**, 148–175 (2012).
30. Xiong, K. N. et al. South China Karst for World Heritage Nomination: Shilin Karst (Yunnan), Libo Karst (Guizhou) and Wulong Karst (Chongqing). Beijing: Ministry of Housing and Urban-Rural Development, the People's Republic of China, 2005.
31. Xiong, K. N., Fu, Y. L., Chen, H., Du, F. J., Xiao, S. Z., et al. South China Karst (Phase II) : Guilin Karst, Shiping Karst, Jinfoshan Karst and Huanjiang Karst. Beijing: Ministry of Housing and Urban-Rural Development, the People's Republic of China; 2013. (in Chinese).
32. Straede, S. & Treue, T. Beyond buffer zone protection: a comparative study of park and buffer zone products' importance to villagers living inside Royal Chitwan National Park and to villagers living in its buffer zone. *J. Environ. Manag.* **78**, 251–267 (2006).
33. Woodward, S. C. & Cooke, L. *World Heritage: concepts, management and conservation* (Taylor & Francis, 2022).
34. Chen, L. et al. How do natural and socio-economic factors influence the sustainable development of the ecological environment in the World Natural Heritage Sites? Evidence from the Jiuzhaigou, China. *J. Clean. Prod.* **428**, 139238 (2023).
35. Fei, G. Y., Xiong, K. N., Fei, G. H., Zhang, H. P. & Zhang, S. H. The conservation and tourism development of World Natural Heritage sites: the current situation and future prospects of research. *J. Nat. Conserv.* **72**, 126347 (2023).
36. Su, M. M., Wall, G. & Xu, K. J. Tourism-induced livelihood changes at mount Sanqingshan world heritage site, China. *Environ. Manag.* **57**, 1024–1040 (2016).
37. Chen, G. L. et al. Bibliometric analysis of spatial technology for world heritage: application, trend and potential paths. *Remote Sens.* **15**, 4695 (2023).
38. Zhang, M., Xiong, K. N., Wang, X. & Zhao, X. Natural beauty and esthetic value of natural world heritage sites: a literature review and implications for Karst Geoheritage Sites. *Geoheritage* **14**, 84 (2022).
39. Xiong, K. N., Li, G. C. & Wang, L. Y. Study on the protection and sustainable development of South China karst Libo world natural heritage site. *Chin. Gard.* **28**, 66–71 (2012).
40. Wang, L. & Xiao, S. Z. Tourism space reconstruction of a world heritage site based on actor network theory: A case study of the Shiping Karst of the South China Karst World Heritage Site. *Int. J. Geoheritage Parks* **8**, 140–151 (2020).
41. Murszewski, A. et al. Regional geological formation and speleogenesis of the 'Fossil Hominid Sites of South Africa' UNESCO world heritage site. *Earth-Sci. Rev.* **188**, 498–513 (2019).
42. Fang, R. N., Zhang, J., Xiong, K. N., Woo, K. S. & Zhang, N. Influencing factors of residents' perception of responsibilities for heritage conservation in world heritage buffer zone: a case study of libo karst. *Sustainability* **13**, 10233 (2021).
43. Zhang, N., Xiong, K. N., Zhang, J. & Xiao, H. Evaluation and prediction of ecological environment of karst world heritage sites based on google earth engine: a case study of Libo-Huanjiang karst. *Environ. Res. Lett.* **18**, 034033 (2023).
44. Zhang, Z. Z., Xiong, K. N., Huang, D. H., Zhang, W. X. & Chang, H. H. Spatial Zoning of the value realization models for ecological products in shiping karst natural world heritage site. *Forests* **14**, 1449 (2023).
45. Phinzi, K. & Ngetar, N. S. The assessment of water-borne erosion at catchment level using GIS-based RUSLE and remote sensing: a review. *Int. Soil Water Conserv. Res.* **7**, 27–46 (2019).
46. Jiang, N. et al. Estimating the soil erosion response to land-use change using GIS-Based RUSLE and remote sensing: a case study of Heilongjiang Province, China. *Sustainability* **15**, 8004 (2023).
47. Mengist, W., Soromessa, T. & Feyisa, G. L. Landscape change effects on habitat quality in a forest biosphere reserve: Implications for the conservation of native habitats. *J. Clean. Prod.* **329**, 129778 (2021).
48. Bai, X., Xiong, K. N., Chen, Y. & Liu, Z. Q. Spatiotemporal evolution of landscape stability in World Heritage Karst Sites: a case study of Shiping Karst and Libo-Huanjiang Karst. *Herit. Sci.* **12**, 215 (2024).
49. Xie, H. L. Regional ecological risk analysis based on landscape structure and spatial statistics. *Ecology* **10**, 5020–5026 (2008).
50. Shi, Y. H., Li, J. Q. & Xie, M. Q. Evaluation of the ecological sensitivity and security of tidal flats in Shanghai. *Ecol. Indic.* **85**, 729–741 (2018).
51. Zhang, X. D., Wang, X. D., Zhou, Z. X., Li, M. W. & Jing, C. G. Spatial quantitative model of human activity disturbance intensity and land use intensity based on GF-6 image, empirical study in Southwest Mountainous County, China. *Remote Sens.* **14**, 4574 (2022).
52. Liu, J. Q., Li, Y. Z., Zong, M., Zhang, B. H. & Wu, X. Q. Changes in human disturbance intensity and its response to landscape pattern in the Yellow River Delta. *J. Earth Inf. Sci.* **20**, 1102–1110 (2018).
53. Liu, S. L. et al. Quantitative evaluation of human activity intensity in the study of regional ecological effects. *Ecology* **38**, 6797–6809 (2018).
54. Zhao, J. C., Ji, G. G., Tian, Y., Chen, Y. L. & Wang, Z. Environmental vulnerability assessment for mainland China based on entropy method. *Ecol. Indic.* **91**, 410–422 (2018).
55. Chirico, G. B., Borga, M., Tarolli, P., Rigon, R. & Preti, F. Role of vegetation on slope stability under transient unsaturated conditions. *Procedia Environ. Sci.* **19**, 932–941 (2013).

56. Xiong, K. N., He, C., Zhang, M. S. & Pu, J. B. A new advance on the improvement of forest ecosystem functions in the karst desertification control. *Forests* **14**, 2115 (2023).

57. Wang, M. W. Calculation of sensitive factors in ecologically sensitive areas of plateau: comprehensive evaluation of ecological carrying capacity. *Appl. Nanosci.* **13**, 1–12 (2021).

58. Hou, K., Li, X. X., Wang, J. J. & Zhang, J. Evaluating ecological vulnerability using the GIS and Analytic Hierarchy Process (AHP) Method in Yan'an, China. *Polish J. Environ. Stud.* **25**, 599–605 (2016).

59. Chen, Y., Xiong, K. N., Ren, X. D. & Cheng, C. Vulnerability comparison between karst and non-karst nature reserves—With a special reference to Guizhou province, China. *Sustainability* **13**, 2442 (2021).

60. Jiang, H. Y. & He, G. Analysis of spatial and temporal evolution of regional water resources carrying capacity and influencing factors—Anhui Province as an example. *Sustainability* **15**, 11255 (2023).

61. Dai, J. P. & Khan, Y. A. Ecological environment pressure state and response system for coupling coordinate development: an application on china data. *Environ. Sci. Pollut. Res.* **30**, 25682–25690 (2023).

62. Liu, K., Yang, S. W., Zhou, Q. & Qiao, Y. R. Spatiotemporal evolution and spatial network analysis of the urban ecological carrying capacity in the Yellow River Basin. *Int. J. Environ. Res. Public Health* **19**, 229 (2021).

63. Zhang, W. F., Xiong, K. N., Li, Y. Y., Song, S. Z. & Xiang, S. Improving grassland ecosystem services for human wellbeing in the karst desertification control area: Anthropogenic factors become more important. *Sci. Total Environ.* **946**, 174199 (2024).

64. He, L. X., Zhang, J., Yu, B., Hu, M. S. & Zhang, Z. H. Assessment of ecosystem health and driving forces in response to landscape pattern dynamics: the Shibing Karst world natural heritage site case study. *Herit. Sci.* **12**, 182 (2024).

65. Ye, S. A., Du, F. J., Wu, K. H. & Liu, Y. H. Participation of Rural Communities in Tourism Development and Its Mechanisms in World Heritage Sites—The Case of Shi Bing Karst[J]. *China Agric. Resour. Zoning* **43**, 294–302 (2022).

66. Zhao, W. Q., Zhou, W. L. & Zhang, F. Study on the dynamic change of vegetation cover in the Yuntai Mountain area of Shibing over the past 40 years. *Res. Soil Water Conserv.* **22**, 241–245 (2015).

67. Xiong, K. N., Li, G. C. & Wang, L. Y. Conservation and sustainable development of Libo World Natural Heritage Site in Southern China Karst. *China Gard.* **28**, 66–71 (2012).

68. Bai, Z. F., Han, L., Liu, H. Q., Liu, L. Z. & Jiang, X. H. Applying the projection pursuit and DPSIR model for evaluation of ecological carrying capacity in Inner Mongolia Autonomous Region, China. *Environ. Sci. Pollut. Res.* **31**, 3259–3275 (2024).

69. Chen, X. D., Yang, Z. P., Wang, T. & Han, F. Landscape ecological risk and ecological security pattern construction in world natural heritage sites: a case study of Bayinbuluke, Xinjiang, China. *ISPRS Int. J. Geo-Inf.* **11**, 328 (2022).

70. Chen, L. et al. Investigation on the spatial and temporal patterns of coupling sustainable development posture and economic development in World Natural Heritage Sites: a case study of Jiuzhaigou, China. *Ecol. Indic.* **146**, 109920 (2023).

71. Chen, Y., Xiong, K. N., Ren, X. D. & Cheng, C. An overview of ecological vulnerability: a bibliometric analysis based on the Web of Science database. *Environ. Sci. Pollut. Res.* **29**, 12984–12996 (2022).

72. Gu, X. Y., Xiong, K. N., Zhang, J. & Chen, H. A comprehensive analysis on integrity conservation of world natural heritage site and buffer zone tourism development with an implication for karst heritage sites. *Geoheritage* **15**, 8 (2023).

73. Xiong, K. N., Zhang, S. R., Fei, G. Y., Jin, A. & Zhang, H. P. Conservation and sustainable tourism development of the natural world heritage site based on aesthetic value identification: a case study of the Libo Karst. *Forests* **14**, 755 (2023).

74. Zhang, J. et al. Exploring the synergy between Karst World Heritage site's OUV conservation and buffer zone's tourism industry development: a case study of the Libo-Huanjiang Karst. *Herit. Sci.* **11**, 202 (2023).

75. Zhang, Y., Zhang, Z. H., Zhang, M. S. & Yuan, Z. W. The global situation of karst desertification research based on forest ecology. *Forests* **15**, 126 (2024).

76. Liu, Q. Q. et al. Quantitative assessment of ecological assets in the world heritage karst sites based on remote sensing: with a special reference to South China Karst. *Herit. Sci.* **12**, 129 (2024).

77. Castillo-Manzano, J. I., Castro-Nuño, M., Lopez-Valpuesta, L. & Zarzoso, Á. Assessing the tourism attractiveness of World Heritage Sites: the case of Spain. *J. Cultural Herit.* **48**, 305–311 (2021).

78. Zhang, J., Xiong, K. N., Liu, Z. J. & He, L. X. Research progress and knowledge system of world heritage tourism: a bibliometric analysis. *Herit. Sci.* **10**, 42 (2022).

79. Aziz, N. A. A., Ariffin, N. F. M., Ismail, N. A. & Alias, A. Community participation in the importance of living heritage conservation and its relationships with the community-based education model towards creating a sustainable community in Melaka UNESCO world heritage site. *Sustainability* **15**, 1935 (2023).

80. Conraddin, K. & Hammer, T. Making the most of world natural heritage—linking conservation and sustainable regional development? *Sustainability* **8**, 323 (2016).

81. Xu, L. L., Yu, H. & Zhong, L. S. Evolution of the landscape pattern in the Xin'an River Basin and its response to tourism activities. *Sci. Total Environ.* **880**, 163472 (2023).

82. Pan, J. Y. Research on Sustainable Tourism Development of Wulong Karst World Natural Heritage Site Based on Tourism Ecological Footprint Model. Chongqing Technology and Business University; 2014. (in Chinese).

83. Zhang, Z., Hu, B. Q., Jiang, W. G. & Qiu, H. H. Spatial and temporal variation and prediction of ecological carrying capacity based on machine learning and PLUS model. *Ecol. Indic.* **154**, 110611 (2023).

Acknowledgements

We appreciate the anonymous reviewers for their invaluable comments and suggestions on this manuscript. This work was supported by China Overseas Expertise Introduction Program for Discipline Innovation (Grant No. D17016), Guizhou Provincial Key Technology R&D Program (No. 220 2023 QKHZC) and the Project of Geographical Society of Guizhou Province (No. GS44-20041218).

Author contributions

M.X. and K.X. developed the concept of this work. M.R.X. wrote the manuscript, K.X. and Y.C. reviewed the whole text and made comments and suggestions to improve it. M.X. was involved in collecting data and producing some of the images. All authors read and approved the final manuscript.

Competing interests

The authors declare no competing interests.

Additional information

Correspondence and requests for materials should be addressed to Kangning Xiong.

Reprints and permissions information is available at <http://www.nature.com/reprints>

Publisher's note Springer Nature remains neutral with regard to jurisdictional claims in published maps and institutional affiliations.

Open Access This article is licensed under a Creative Commons Attribution-NonCommercial-NoDerivatives 4.0 International License, which permits any non-commercial use, sharing, distribution and reproduction in any medium or format, as long as you give appropriate credit to the original author(s) and the source, provide a link to the Creative Commons licence, and indicate if you modified the licensed material. You do not have permission under this licence to share adapted material derived from this article or parts of it. The images or other third party material in this article are included in the article's Creative Commons licence, unless indicated otherwise in a credit line to the material. If material is not included in the article's Creative Commons licence and your intended use is not permitted by statutory regulation or exceeds the permitted use, you will need to obtain permission directly from the copyright holder. To view a copy of this licence, visit <http://creativecommons.org/licenses/by-nc-nd/4.0/>.

© The Author(s) 2025